Materials and Design 111 (2016) 165–173

Contents lists available at ScienceDirect

Materials and Design

journal homepage: www.elsevier.com/locate/matdes

Laser cladding: The alternative for field thermite welds life extension

F.C. Robles Hernández [a,b,*], A.O. Okonkwo [a], V. Kadekar [c], T. Metz [1], N. Badi [b,d]

[a] University of Houston, College of Technology, 4730 Calhoun Rd., Houston, TX 77204, USA
[b] Center for Advanced Materials, University of Houston, Houston, TX 77204-5004, USA
[c] Oerlikon Metco (US) Inc - Laser Cladding Services, Houston, TX 77040, USA
[d] Department of Physics, College of Science, University of Tabuk, P.O. Box 741, Tabuk 71491, Saudi Arabia

HIGHLIGHTS

- This is a successful attempt for laser cladding coatings applications for full scale testing under heavy haul environment,
- The combination of testing and materials design improved the laser cladding in up to 1400% with respect with previous work,
- Heat treatment protocols have demonstrated to be the accurate path to hinder or temper martensite and to improve toughness,
- The heat treatments protocol is useful to tune hardness,

GRAPHICAL ABSTRACT

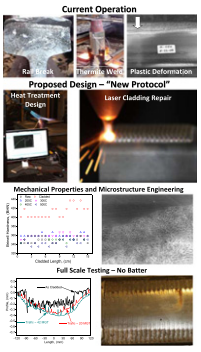

ARTICLE INFO

Article history:
Received 1 May 2016
Received in revised form 19 August 2016
Accepted 22 August 2016
Available online 27 August 2016

Keywords:
High carbon steel
Laser cladding
Heat treatment design
Railways
Instrumented jominy test

ABSTRACT

Thermite field welds are the link of rails; however, they experience plastic deformation (batter) along the area above the heat affected zone (HAZ). Here we present the benefits of using laser cladding to minimize the plastic deformation on the HAZ. Our test consisted of a laboratory and a full scale approach under the most extreme revenue service conditions known in North America. The laser cladding coatings were used in the past for rails but its life was terminated in their infancy (after approximately 3–4 MGT) due to the presence of un-tempered martensite that negatively affected the rail toughness. The new tested laser cladding design is capable of producing a sound coating with tunable hardness (from 360–430 HBN). This is possible through a new heat treatment procedure carried using a propane torch or induction heating at temperatures between 400 and 500 °C and cooling rates below 3 °C/s. The microstructure shows that the rail after laser cladding is fully pearlitic. The laser cladded welds sustained up to 42 million gross tons in heavy haul traffic that is between 1000 and 1400% improvement when compared to other previous works.

Published by Elsevier Ltd.

1. Introduction

Field welds (e.g. thermite welds) are one of the weakest links in the rail tracks and when they failing they generate catastrophic or unsafe conditions [1–4]. The weld breaks are usually repaired by adding a rail section, also known as plug, that is thermite welded in both ends. This increases the number thermite welds in the

* Corresponding author at: University of Houston, College of Technology, 4730 Calhoun Rd., Houston, TX 77204, USA.
E-mail address: fcrobles@uh.edu (F.C. Robles Hernández).
[1] Supported this project while he was at Laser Cladding Services.

http://dx.doi.org/10.1016/j.matdes.2016.08.061
0264-1275/Published by Elsevier Ltd.

field and compromises the rail life expectancy and the track's integrity[2] [5,6]. Thermite welds, particularly at the Heat Affected Zone (HAZ), experience undesirable plastic deformation known as batter (Fig. 1). Batter is one of the causes of premature failures and rail removal. The HAZ is a weak spot with a sharp reduction in hardness resulting from localized annealing [7–9]. The microhardness along the HAZ decreases in up to 140 μHV (from 380 μHV to 240 μHV). The decrease in hardness is the result of changes in microstructure in the corresponding locations as shown in Fig. 1(f-g). The parent rail is pearlitic with presence of pro-eutectoid cementite and the HAZ is spheroidized pearlite that is well known for its rather softer nature.

For 50 years the rail has improved considerably, as an example the hardness improved from 248 HBN to more than 400 HBN [10]. This accomplishment is mainly attributed to new metallurgies and heat treatments. Yet, this did not solve the batter problem that it is still observable along the HAZ. Other laser techniques that have been used for rail applications include: laser glazing and the LISI process [11–15]. Additionally, some of the effective methods for rail life extension include top of rail lubrication and rail grinding [16]. But unfortunately, they have unappreciable effect, if any, to hinder the effects of batter.

A major drawback in the use of laser treatments on rails is the formation of martensite that it is certainly a hard phase, which may have benefits for wear resistance [17–19]. Regrettably, un-tempered martensite, is brittle and therefore it is not suitable for environments under dynamic loading and high impacts [7,20–23]. Laser cladding is a well known method having a wide variety of industrial applications. However, its industrial implementation for the railways has not been optimized that is a major goal of this research paper. Here we are proposing a new process designs for laser cladding [24–26] coatings to retain martensite or to post-treat it (tempering) and make it effective for the railroads. Fig. 1 sketches the thermite welds process and shows a rail with the batter or plastic deformation typically observed over the HAZ area. The respective microstructures are also included and show the typical pearlitic microstructure in the parent rail. On the other hand, the microstructure in the HAZ is spheroidized pearlite. Further details about the effects of various type of rail welding can be consulted in [27].

Here we present metallurgical and field test results of rails treated with the use of laser cladding coatings to prevent the negative effects of batter caused along the HAZ. New rail alloy design can be an alternative to improve rails; however, it is time consuming, labor intensive, expensive and may not necessarily eliminate batter [28–30]. Therefore, this alternative method is made to prevent weld failure.

Fig. 2 shows the system used to deposit the laser cladding coatings and the in-line thermal analysis system that is the key to monitor the pre-heating, cooling, and post-treatment processes to tune the microstructure and properties. This approach serves to design the heating and cooling procedures. The heating and cooling is closely monitored and investigated by means of advanced thermal analysis, and instrumented Jominy test samples [31,32], metallography, and numerical simulations. This complementary combination of tools is key to develop the new laser cladding protocol for railroad applications. Once the phase transformations are understood (based on thermal analysis) a final cooling rate or heat treatment protocol is design to optimize the final hardness and microstructure. The final product should meet the requirements stated in the AREMA recommended practices.

For the purpose of full scale testing, we produced 6 welds, 2 of them were used for laboratory testing and the other four were installed in track for full scale testing at the track known as FAST (Facility for Accelerated Service Testing [33–35]). FAST is a unique laboratory and well controlled environment at the Transportation Technology Center, Inc. (TTCI) that is a facility situated in Pueblo Colorado, USA. This is a full scale railway facility with a track of 4.4 km and an axle load of 39-tons. TTCI has an axle loading environment that is above the North American standards for revenue service with the intention to accelerate testing.

[2] http://onlinepubs.trb.org/onlinepubs/tcrp/tcrp_rpt_155.pdf.

2. Experimental procedure

The composition of the laser cladding coating is in Table 1. This composition was selected from a large number of alloys. The selection of the alloy was carried based on its superior properties, and most importantly, its resistance to cracking during cooling. Fig. 3 shows examples of microstructures of coatings with and without cracks. In Fig. 3c is observed a fully martensitic microstructure. Both, the cracks and the martensite are attributed to the rapid cooling. Other tested powder compositions are given in reference [7]. The laser cladding conditions are: wavelength: 900–1080 nm, cladding speed: 800 to 1200 mm/min, power: 1.5 to 2 kW, pre-heat: 400–450 °C.

The instrumented Jominy is design with a 5 mm bore from the top of the sample to 3–4 mm from the bottom end. The instrumented Jominy samples are heated to 900 °C for 1.5 h (to reach fully austenitic microstructure) and then cooled under the following three conditions: natural heat exchange (normalizing), compressed air, and water quenching. The exact heating/cooling conditions were determined using a battery of 5 K-type thermocouples inserted in the bore of the jominy sample and the rail during heating and cooling. This set up was used to collect the thermal history of the rail before, during and after cladding.

The heating process is carried based using a propane torch or induction heating system. The heating set-ups are shown in Fig. 2a (torch) and induction (Fig. 4). For the induction heating the power is supplied to the coil via an electric transformer and a Variac with a total power output of 1 kW. The coil is homemade using ¼ inch copper tubing and tap water is allowed to flow as coolant. The transformer is Sigma, model MPI-900 - 10 that operated at 90 A and 10 V as well as 180 A and 5 V. The Variac supplied AC current of 20 A and up to 110 V in serial and parallel configurations. This set-up is efficient for the laboratory experiments, but may need further optimization for in-track use and a power source of least 3 kW. The inductor can be designed using the following algorithm: $\delta = 1/\sqrt{\sigma\mu_o\mu_r f}$; where δ is the depth of penetration [mm], σ is the electric conductivity [Ω/mm^2], μ_o is the absolute permeability, μ_r is the relative permeability and f is the frequency (ideally 100–400 kHz).

3. Full scale test

The FAST conditions for the full-scale rail performance testing facility include a loop of 4.4 km, the full scale train or “consist” has more than 150 cars and 4 locomotives for an approximate length of 1.5+ km. Each 150 cars are loaded with 143 tons that is equivalent to 39 tons per axel. The consist runs approximately 440 km (100 laps) per day accumulating approximately 1.5 megatons (MGT). The axle load at FAST is the most extreme rail testing environment in North America and was selected for its accuracy and speed to obtain reliable/full scale test results.

4. Results

The Jominy test is summarized in Fig. 5 where it is possible to observe the cooling behavior of the investigated steels cooled under different environments. The cooling history is collected to identify the exact conditions (temperature and time) at which the phase transformations occur. Further understanding is carried in the cooling curve's first derivatives where the slop changes enhance the phase transformations. The integral of the first derivative is a function of the energy required for the transformation to occur that is a direct function of the amount of phase transforming (fraction transforming) [36,37]. Therefore, by

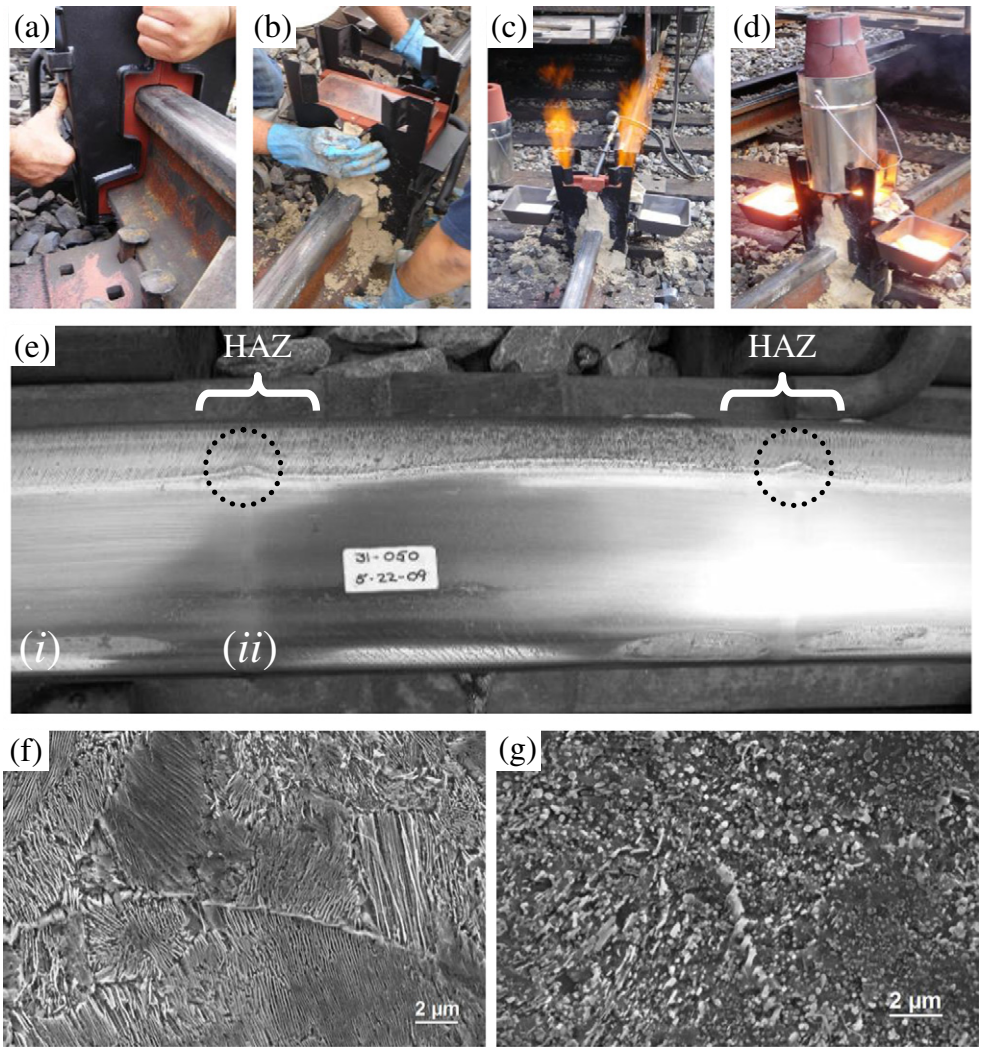

Fig. 1. Thermite Welding Process on the field (a) molding, (b) sand sealing (liquid metal leak prevention), (c) preheating (cold spot prevention), (d) initiation of the thermal welding, and (e) rail tested in the field showing plastic deformation or batter near the HAZ (see the arrows). Representative microstructures for the (f) parent rail and the (g) heat affected zone for the locations identified in (e) with Roman numbers (*i*) and (*ii*) respectively.

measuring the partial integrals (one per phase: pro-eutectoid cementite, pearlite, bainite, and martensite) we can determine the gross amount of each phase (Fig. 5c and f). The first derivatives for all the investigated steels are given in the Supplementary Material (SM 1a,1b). A detail description of the thermal analysis (particularly the partial integrals) is provided in [38–41]. Fig. 6 shows the thermal analysis, and hardenability test results that are used to conclusively to select Steel 1.

The two rail metallurgies selected are the standard (Steel 2) and premium (Steel 1) rails. These rail metallurgies are the most common for heavy haul service in North America. Here we observe that Steel 1 offers several advantages such as an almost fully pearlitic microstructure and limited martensite formation. Additionally, Steel 1 has higher hardenability than that in Steel 2. Therefore, this rail expected to have superior wear resistance and hence longer life. High carbon steels have the tendency to produce pro-eutectoid cementite, which may be hard, but definitely not the most recommended phase for rail applications due to its negative effects on fracture toughness. The presence of this phase in Steel 1 is limited and can be hindered by proper cooling. In fact, this phase is not visible in Figs. 6b,c that is attributed to the cooling conditions. Steel 1 has higher tendency for martensite retention that complies with the AREMA recommended practices [42]. The amount of martensite in Steel 2 result excessive residual stresses and cracking in the water quenched sample (see insets in Fig. 6d). The cracking tendency in high carbon steels is well documented [43,44]. High carbon steels are well known for their tendency to form martensite [45], which as mentioned before it is not recommended for rail applications [42]. Yet, here is important to show that the carbon content in Steel 1 is larger than in Steel 2, but due to its superior allow design, presumably low manganese [46,47], it is more resistant to martensite formation.

The instrumented Jominy sample allowed a rapid identification of the best cooling practice for the investigated steels. This tool is important because it does allow to identify not only the exact temperature at which each phase precipitates, but also the cooling rate to promote or hinder such phase. The combination of the heating and cooling environments used herein is ideal to have a wide spectrum of conditions to identify the optimum for rail applications. Both, compressed air and water were applied as recommended by Jominy test [48]. The hardness results and the respective microstructures for the investigated steels are presented in Fig. 6.

In the microstructure of Steel 1 that was water quenched are observed traces of martensite; however, the amount is limited and hard to observe as seen in Fig. 6b. The metallurgical bonding among the rail

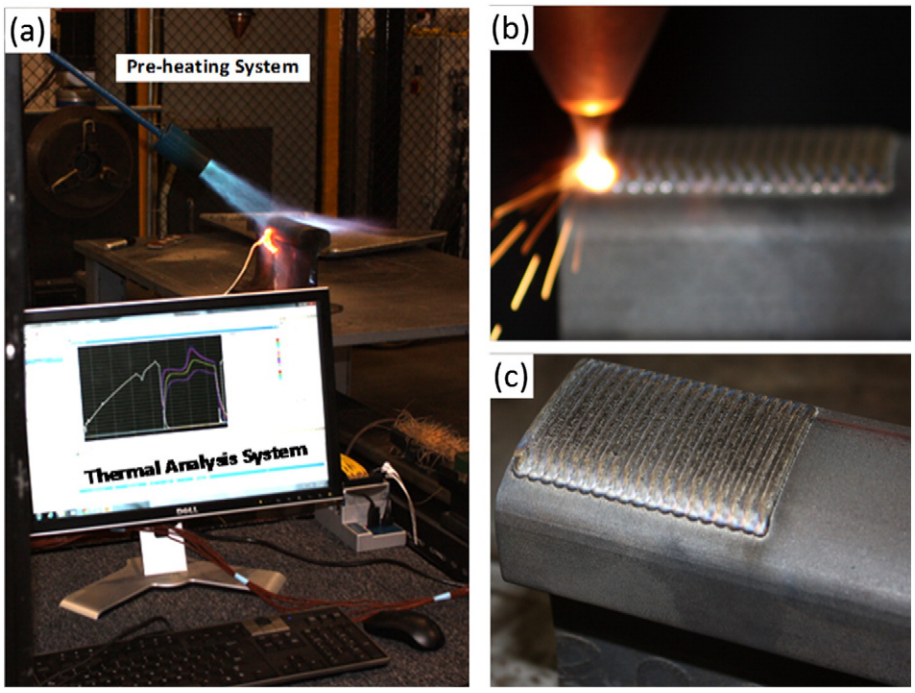

Fig. 2. Example of the laser cladding process (a) the pre-heating and thermal analysis workstation (b) Laser Cladding process and (c) cladded surface of the rail after the coating.

and the coating is the result of melt fusion, which is satisfactorily deposited along the rail and developed a proper cladding coating with a true metallurgical bond. In this procedure we identified the right heating and cooling conditions for the laser cladding for Steel 1. In the event that the rail was cooled faster than the ideal conditions, there is a possibility to eliminate any un-tempered martensite via post-treatment (tempering) to tune and refine the final microstructure and mechanical properties. In order to further succeed in this we simulated the continuous cooling transformation (CCT) diagram shown in Fig. 7.

Fig. 7 shows the critical temperatures and cooling rates to obtain a fully pearlitic microstructure in Steel 1. The simulated diagram is made using the exact composition of Steel 1. The dotted continuous cooling curve shows that the maximum cooling rate for Steel 1 to prevent martensite formation. This cooling rate is approximately 2 °C/s. The same cooling rate allows to transform the microstructure into a fully pearlitic that is the recommended microstructure by AREMA [49]. In order to reach the right microstructure the rail needs to cool down from 750 °C (austenitic temperature) to 400 °C in approximately 3 min.

During the laser cladding the rail reaches heating temperatures above austenitic conditions. Therefore, it is necessary to cool the rail carefully to reach the highest possible hardness, but preventing a sudden drop in temperature (below 200 °C) that may promote martensite. The major problem here is the different masses and temperature gradients among the coating and the rail. The larger mass in the rail's head and lower temperature works as a heat sink extracting the heat from the coating rapidly. In the event that the rail is allow to cool naturally after the coating the microstructure in the vicinity is transformed into martensite. Therefore controlled cooling may be needed for laser cladding use for rail applications. Under some circumstances a refractory blanket may be enough to reach this cooling environment.

A successful laser cladding treatment is shown in Fig. 8 where a perfect fusion among the rail and coating is observed. This is possible by proper cooling. For rapid optimization we suggest induction heating as it can be automated. Unfortunately this method may represent challenges with respect to system design and timelines to access the track. The alternative is torch heating that can be set aside and use even during traffic. Yet, this alternative may be restricted in some areas where open flames in revenue services are forbidden. In our experience both methods work and their implementation will depend purely upon the needs, safety, and accessibility to the track or restrictions established by the railway.

Fig. 8c shows the hardness results made approximately 5 mm below the cladded coating in a 15 cm long section. This data covers from one end to the other end of the coated section of the rail. As observed in this figure the hardness values are comparable to those expected at this depth by AREMA recommended practices [49]. The measurements were made in Rockwell C scale and converted into Brinell hardness using the hardness conversion algorithm proposed by AREMA [49].

An example of a rail cooled under natural heat exchange conditions following the laser cladding coating are presented in Fig. 8c. In this case the microstructure is martensitic. The hardness in is tuned with the assistant of the tempered (post-treated) sample demonstrate that martensite can be treated to eliminate un-tempered martensite. The effects of martensite tempering are well known and usually result in toughness improvements [50,51]. The post-treatment demonstrates that temperatures as low as 200 °C are effective to temper the martensite in only 10 min. Although, the martensite tempering is

Table 1
Chemical composition, in wt%, of the laser cladding powders.

Element	C	Ni	Mn	Cr	Si	B	Fe
Coating	1.3	35.0	0.7	9.5	2.0	0.9	Balance
Steel 1	1.0	0.02	0.0	0.22	0.44	0.0	Balance
Steel 2	0.92	0.11	1.04	0.20	0.37	0.0	Balance

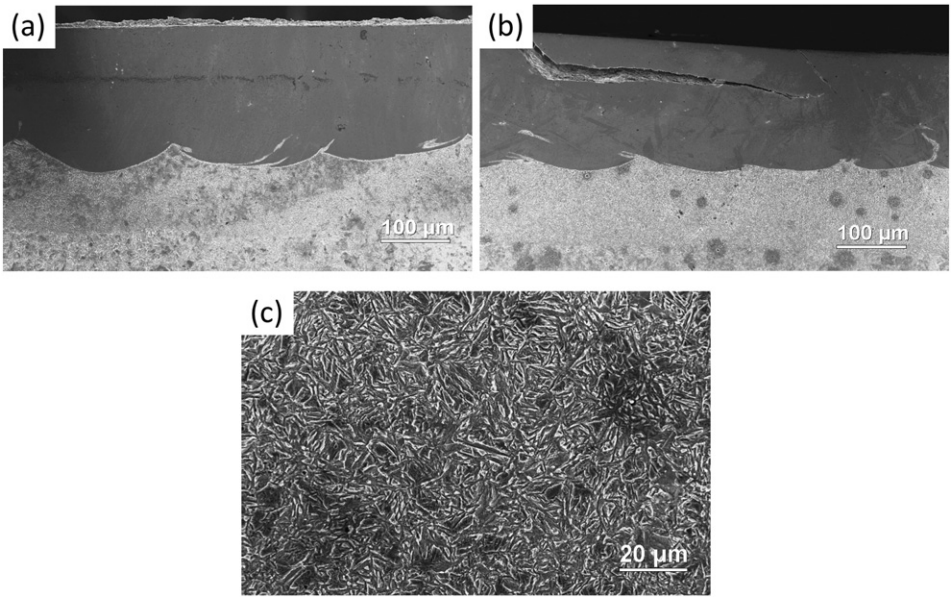

Fig. 3. Microstructures of the cross sections of the rail showing the (a–b) cladding coating and (c) the martensitic microstructure of the parent rail in the vicinity of the cladded area showing a fully martensitic structure. In (a) is presented a crack free coating and in (b) a coating with the typical cracks.

not expected to be the standard procedure for rail applications, it can be used as an alternative procedure. The best practice is definitely controlled heating/cooling.

The dye penentrants or non-destructive analysis of the rails tested at FAST before and after service are presented in Fig. 9. This figure shows that the laser cladded rails can be manufactured without cracking, which is a major finding in this work. Cracked coatings on rails limit their implementation for revenue applications. This crack suppression was possible by a proper pre-heating and cooling of the rail prior, during and post-laser cladding application. The ideal pre-heating temperature for Steel 1 is between 400 and 450 °C, but this temperature may change with the cladding material and rail metallurgy. The exact temperature for other metallurgies can be determined using the Jominy test and continuous cooling transformation diagram. Once the welds were installed in service we observed a cracking network after approximately 1.5 MGT. Nevertheless, no crack grow was observed in the following 37 MGT for a total of 42 MGT (Fig. 9c and d).

The integrity of the tested welds was monitored daily using dye penetrants to confirm its compliance with service operations. The most significant results are presented in Fig. 9. The cracks revealed by dye penetrants were unexpected, but the test was allowed to continue under close monitoring. The reason to continue the test is that using other non-destructive testing (NDT) such as ultrasound was demonstrated that the cracks were present along the surface, having limited to no interaction in the parent rail. The full scale testing was considered safe to continue. The continuous NDT testing demonstrated that the cracks did not present further damage.

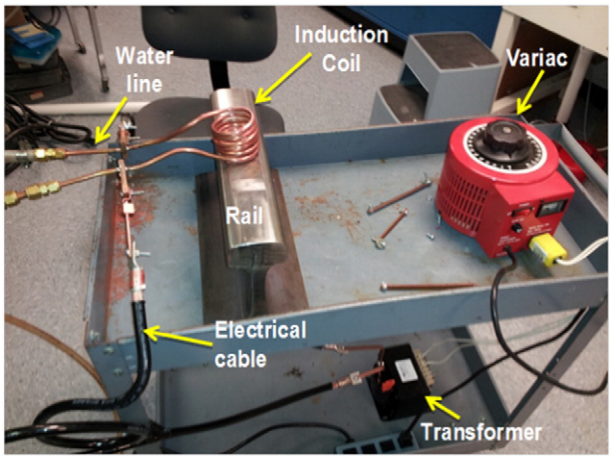

Fig. 4. Experimental setup of the inductive heater for rails.

5. Batter analysis

The Miniprof® profilometer results show the cladded rail in the as cladded, 20 MGT and 42 MGT of traffic. The changes in the profilometer measurements show that the traffic has minor effects on plastic deformation of the rail. In Fig. 10 is observed that after 42 MGT of traffic the plastic deformation is less than 0.3 mm, which is considered negligible. This deformation occurred evenly along the weld rather than localized at the HAZ. This demonstrates that there is no HAZ effect on the coating. It is certain that the tested welds show a few cracks under dye penetrants; however, the welds presented herein sustained between 10 and 14 times more traffic than other welds tested using similar processing methods, including other laser technologies. The results presented in this manuscript and this newly design technology clearly demonstrate potential for revenue service use.

6. Discussion

In previous tests the use of laser methods (including laser cladding) showed success to deposit the layer of the material over the rail. Regrettably, due to an inappropriate cooling the coating did not resist more than 3–4 MGT before it delaminates excessively, which compromised

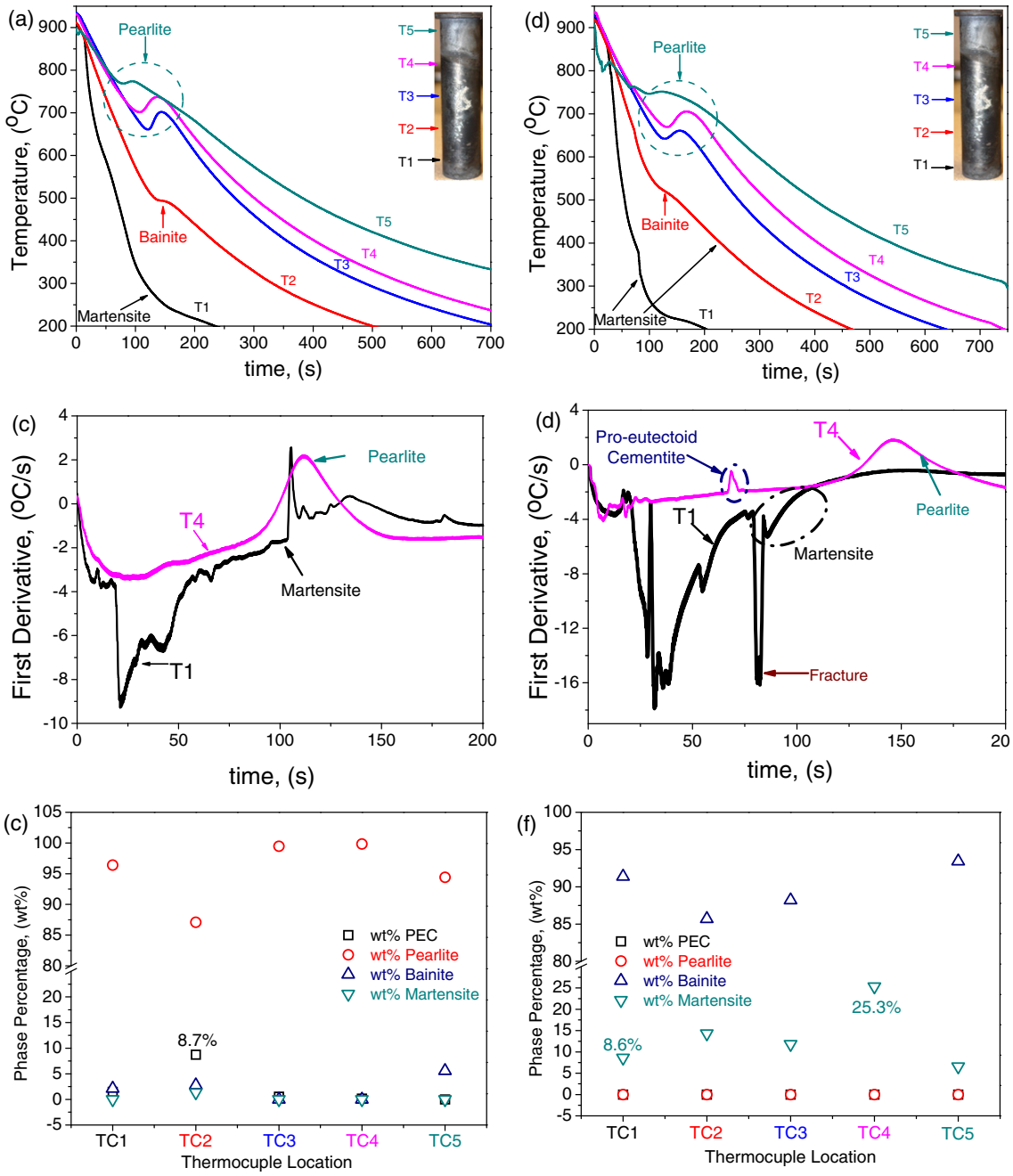

Fig. 5. Results of instrumented Jominy test samples using thermal analysis for (a, b, c) Steel 1 and (d, e, f) Steel 2 samples. In (a, d) are provided the cooling curves of the instrumented Jominy test samples, (b, e) provide selected first derivatives for thermocouple 1 and 4 (T1 and T4 respectively), and (c, f) has the phase analysis. The T1–T5 points to the relative location where the thermocouple was located.

the track integrity, forcing the immediate removal from the FAST tracks. Here we demonstrated that our proposed protocol is successful to produce sound laser coatings. However, this requires proper heating and cooling prior and post laser cladding process. Furthermore, the experimental/lab results demonstrate that un-tempered martensite can be treated in the field at temperatures as low as 200 °C and for times as short as 10 min. This combination of heat treatments can positively contribute to launch this process for full scale applications in revenue service for rail life extension.

The improvements of the technologies shown in this research work are attractive for welds. We also contemplate that this technology can be used for rail repairs. The benefits are in general attractive, and we oversee potential use in locations where the Fall and Winter prevents welding (e.g. northern USA, Canada, northern Europe) due to excessive residual (tensile) stresses. The residual stresses are the result of a decrease in "neutral temperature" and are the main cause of rail failure during the Fall and Winter. Therefore, this compromises the track and may affect safety. Laser cladding is an alternative method to for rail repair preventing any drops in neutral temperature while the temperature backs up and welding is again recommended.

In the current state the technology is ideal for welds and rail repairs for transit systems or railways, preferably with axel load below those

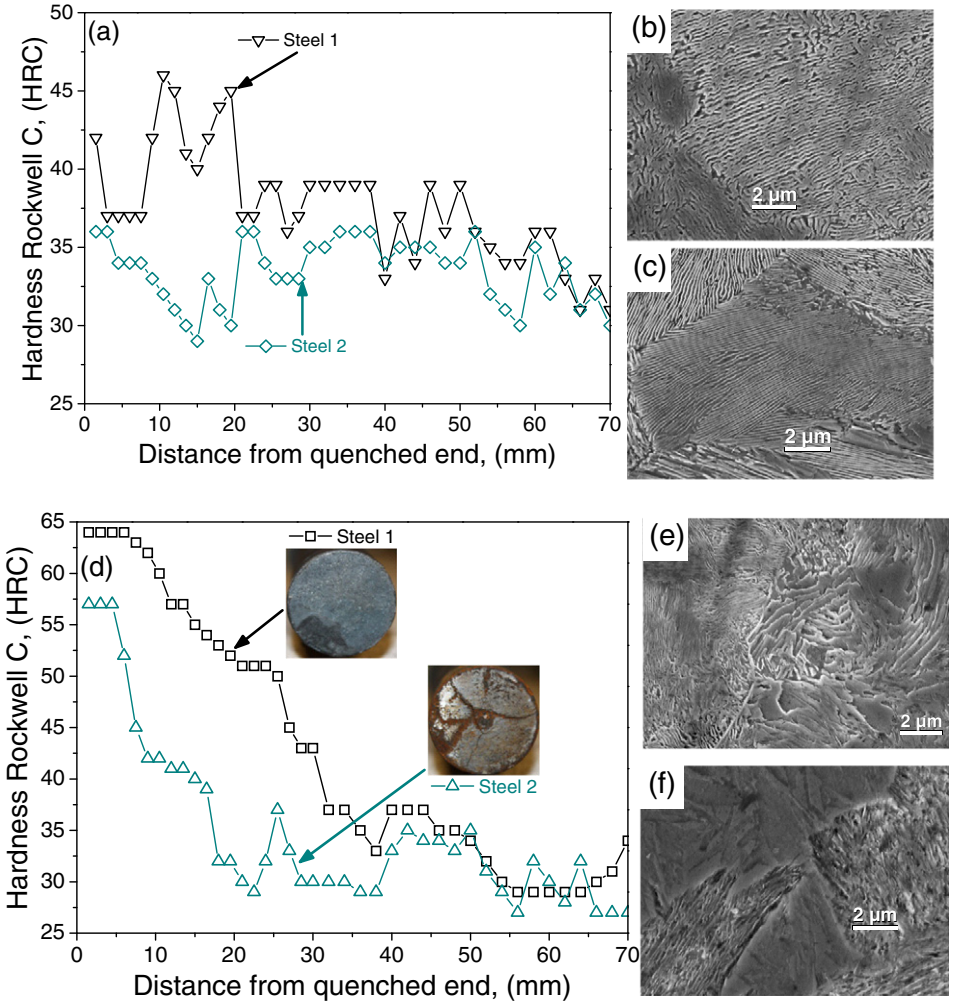

Fig. 6. (a, d) Hardness results of the Jominy test samples cooled under (a–c) air or (d–f) water quenched conditions. The microstructures (b, e) are from Steel 1 and microstructures (c, f) are from Steel 2.

observed at FAST. This technology can be used for all types of rails and it is not unique for premium rail. In the case of standard or other rail metallurgy it will be necessary to design a new heating/cooling protocol. In fact, by investigating other rail metallurgies it is possible to develop a treatment that is useful for all rail metallurgies and it is contemplated for the future work. Currently Laser Cladding is ready for in-shop operations.

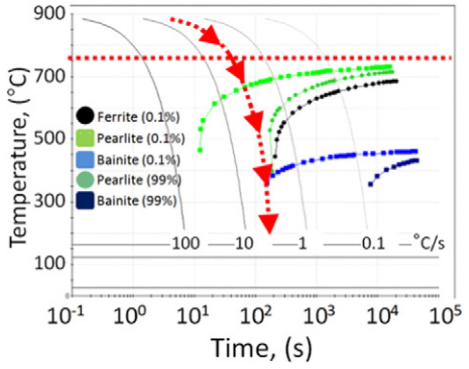

Fig. 7. Simulated continuous cooling transformation diagram for Steel 1. The horizontal red-dotted line is the austenitic isotherm and the dotted continuous cooling curve with the arrows represents the fastest cooling rate to retain martensite.

7. Concluding remarks

Here we presented a methodology to successfully produce laser cladding coatings for railroad applications. The combination of thermal analysis, heat treatment, numerical simulations and mechanical properties demonstrated a complementary set of techniques to optimize laser cladding for railway use. Following this procedure the service life of laser cladded components is improved in up to 1400% when compared to previous attempts tested. The coatings presented herein were successfully tested for up to 42 MGT in a full scale-heavy haul environment with superior axle loading environment to the typical loading environments in revenue service in North American revenue service. A key aspect in the success of this project is the engineering to develop a heating/cooling protocol for coatings using laser cladding for railways applications. This protocol is successful to tune the microstructure and hardness in the rail, which resulted in rail life extension. The heating and cooling environments are accomplished by means of open flame or torch and

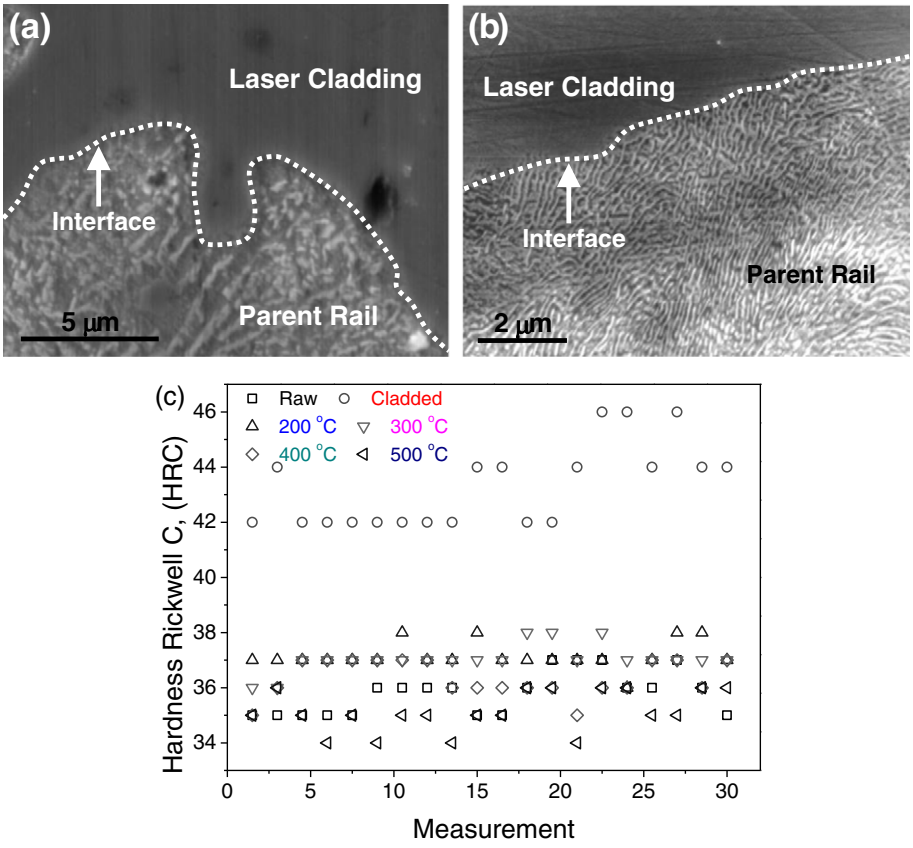

Fig. 8. SEM micrographs of the rails under rail head showing two different cooling environments (a) natural heat exchange conditions and (b) cooled rail by assisted induction heating and (c) hardness changes below the laser cladded surface in the as cladded samples and samples heat treated at various temperatures. Note: in (a) the main microstructure in the parent rail is un-tempered martensite, while for the parent rail in (b) the microstructure is fully pearlitic.

induction heating. The heating/cooling procedures can be designed for a wide variety of steels.

Acknowledgements

FCRH and AOO would like to thank the financial support of National Academies' Transportation Research Board (TRB) IDEA Program funded by the Federal Railroad Administration. The project team is grateful for all the efforts and support from the Transportation Technology Center, Inc. (TTCI) for the field testing particularly Mr. D. Gutscher for facilitating the FAST track for this test.

Appendix A. Supplementary data

Supplementary data to this article can be found online at http://dx.doi.org/10.1016/j.matdes.2016.08.061.

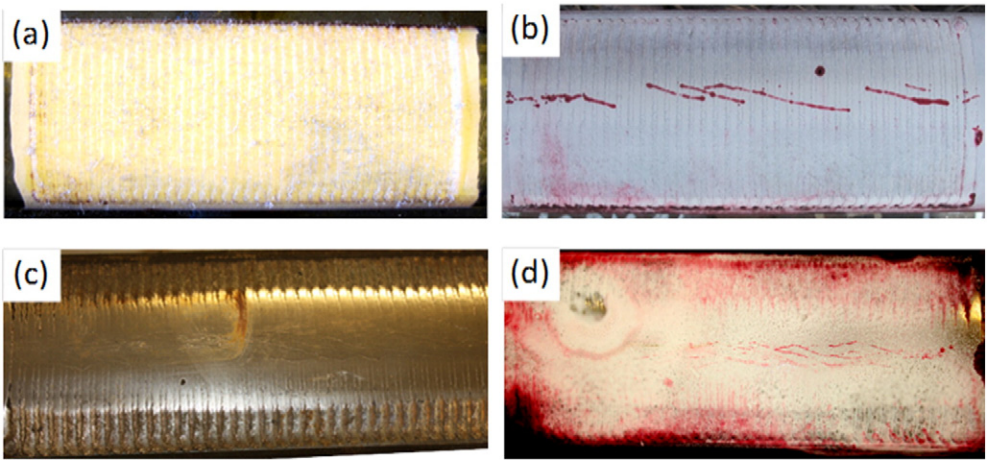

Fig. 9. Dye penetrant testing of the cladded rail in the (a) as manufactured conditions, (b) tested at FAST for 5 MGT, and (c–d) approximately 42 MGT.

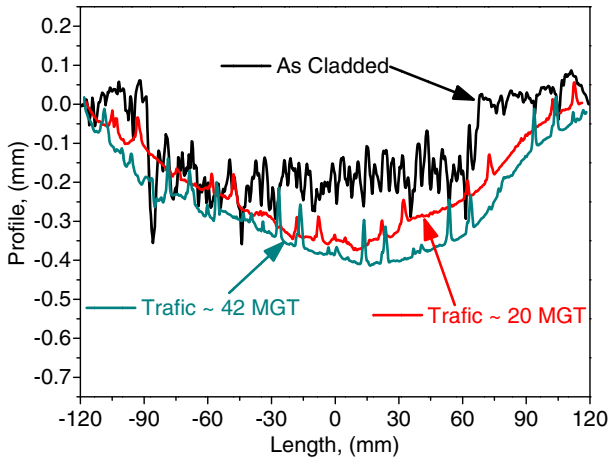

Fig. 10. Miniprof® profiles made along the cladded rails in the as cladded conditions (reference) and after field testing. The set of rails were removed after the indicated traffic (tonnage), but it is important to clarify that neither of both welds fail or represented harsh environments to the FAST operation.

References

[1] L.C. Schroeder, D.R. Poirier, The mechanical properties of thermite welds in premium alloy rails, Mater. Sci. Eng. 63 (1) (1984) 1–21.
[2] M. Burstow, Experience of premium grade rail steels to resist rolling contact fatigue (RCF) on GB network, Ironmak. Steelmak. 40 (2) (2013) 103–107.
[3] K.J. Griffin, G.W. Rosval, In-track assessment of premium and intermediate grade rail steels, CIM Bull. 81 (914) (1988) 117–124.
[4] K.J. Griffin, G.W. Rosval, In-track assessment of premium rail steels, CIM Bull. 80 (902) (1987) 98.
[5] C.J. Lonsdale, Thermite Rail Welding: History, Process Developments, Current Practices and Outlook for the 21st Century Arema Conference Proceedures, **1**(1), 1999 18.
[6] W. Weart, Thermite welding equipment and techniques, Progress. Railr. (2010).
[7] F.C. Robles Hernandez, A.O. Okonkwo, Laser Cladding of Welds to Improve Railroad Track Safety, in Rail Safety IDEA, National Academies, Washintong, D.C., 2015 29.
[8] B. Hanhold, S.S. Babu, G. Cola, Investigation of heat affected zone softening in armour steels part 1-phase transformation kinetics, Sci. Technol. Weld. Join. 18 (3) (2013) 247–252.
[9] H. Zhou, et al., Fatigue evaluation of a composite railway bridge based on fracture mechanics through global–local dynamic analysis, J. Constr. Steel Res. 122 (2016) 1–13.
[10] R. Ordóñez Olivares, et al., Advanced metallurgical alloy design and thermomechanical processing for rails steels for north American heavy haul use, Wear 271 (1–2) (2011) 364–373.
[11] S. Aldajah, Tribological Effect of Laser Glazing and Top of Rail Lubrication on Wheel-Rail Interaction, Illinois Institute of Technology, Chicago, 2003 155.
[12] S. Aldajah, Tribological Effect of Laser Glazing and Top of Rail Lubrication on Wheel-rail Interaction, Illinois Institute of Technology, 2003.
[13] S. Aldajah, et al., Investigation of top of rail lubrication and laser glazing for improved railroad energy efficiency, J. Tribol. 125 (3) (2003) 643–648.
[14] D. Rajput, et al., Molybdenum-on-chromium dual coating on steel, Surf. Coat. Technol. 203 (9) (2009) 1281–1287.
[15] L. Costa, et al., Unique corrosion and wear resistant identification tags via LISI™ laser marking, Surf. Coat. Technol. 203 (14) (2009) 1984–1990.
[16] M. Steenbergen, Rolling contact fatigue in relation to rail grinding, Wear 356–357 (2016) 110–121.
[17] R.F. Barron, Cryogenic treatment of metals to improve wear-resistance, Cryogenics 22 (8) (1982) 409–413.
[18] M.A. Filippov, et al., Effect of heat treatment on the wear resistance of high-carbon and high-nitrogen steels subjected to abrasive wear, Met. Sci. Heat Treat. 48 (3–4) (2006) 170–174.
[19] C. Thaulow, A.J. Paauw, K. Guttormsen, The heat-affected zone toughness of low-carbon microalloyed steels, Weld. J. 66 (9) (1987) S266–S279.
[20] J. Kalousek, D.M. Fegredo, E.E. Laufer, The wear resistance and worn metallography of pearlite, bainite and tempered martensite rail steel microstructures of high hardness, Wear 105 (3) (1985) 199–222.
[21] Gutscher, D., Analysis of Thermite Welds Made in High Carbon Rails, in Technology Digest, TD-10-015., Editor. 2010. , Transportation Technology Center, Inc. and the Association of the American Railroads: Pueblo, CO USA. p. 1-4.
[22] F.C. Robles Hernandez, et al., Mechanical properties and wear performance of premium rail steels, Wear 263 (2007) 766–772.
[23] D.H. Stone, F. Robles, G. Dahlman, Effects of Microvoids, Oxide Inclusions, and Sulfide Inclusions of the Fatigue Strength of Wheel Steels, Proceedings of the Asme/Ieee Joint Rail Conference and the Asme Internal Combustion Engine Division Spring Technical Conference - 2007 2007, pp. 7–11.
[24] J. Lin, W.M. Steen, Design characteristics and development of a nozzle for coaxial laser cladding, J. Laser Appl. 10 (2) (1998) 55–63.
[25] J. Lin, W.M. Steen, Design Characteristics and Development of a Nozzle for Coaxial Laser Cladding, Icaleo'96 - Proceedings of the Laser Materials Processing Conference, 81, 1996, pp. A27–A36.
[26] S. Nowotny, et al., High-performance laser cladding with combined energy sources, J. Laser Appl. 27 (2015).
[27] K. Saita, et al., *Trends in Rail Welding Technologies and Our Future Approach*, Technology, Editor. 2013, NIPPON STEEL & SUMITOMO METAL: Fukuoka. p. 9.
[28] Robles Hernandez, F.C. and D.H. Stone, Railroad wheel steels having improved resistance to rolling contact fatigue, U.P. Office, Editor. 2009, Transportation Technology Center, Inc. (Pueblo, CO): USA. p. 9.
[29] Robles Hernandez, F.C. and D.H. Stone, *Railroad steels having improved resistance to rolling contact fatigue*, U.P. Office, Editor. 2009, Transportation Technology Center, Inc. (Pueblo, CO): USA. p. 9.
[30] F.C. Robles Hernandez, S. Kalay, S. Cummings, Properties and Microstructure of High Performance Wheels, in: T.T. Transfer (Ed.), Technology Digest, Transportation Technology Center, Inc., Pueblo, CO. 2009, p. 4.
[31] A, G.M., Method for determining hardenability of steel. 1951, Google Patents.
[32] P. Le Masson, et al., A numerical study for the estimation of a convection heat transfer coefficient during a metallurgical "jominy end-quench" test, Int. J. Therm. Sci. 41 (6) (2002) 517–527.
[33] R.K. Steele, A perspectival review of rail behavior at the facility for accelerated service testing, Can. Metall. Q. 22 (3) (1983) 353–367.
[34] D.Q. Li, D.N. Bilow, Testing of slab track under heavy axle loads, Transp. Res. Rec. 2043 (2008) 55–64.
[35] S. Kumar, B.R. Rajkumar, Laboratory investigation of wheel rail contact stresses for United-States freight cars, J. Eng. Ind. Trans. ASME 103 (2) (1981) 246–255.
[36] G.O. Piloyan, I. Ryabchik, O.S. Novikova, Determination of activation energies of chemical reactions by differential thermal analysis, Nature 212 (5067) (1966) 1229-&.
[37] A.G. Marangoni, On the use and misuse of the avrami equation in characterization of the kinetics of fat crystallization (vol 75, pg 1465, 1998), J. Am. Oil Chem. Soc. 76 (2) (1999) 281.
[38] F.C. Robles Hernandez, J.H. Sokolowski, Comparison among chemical and electromagnetic stirring and vibration melt treatments for Al-Si hypereutectic alloys, J. Alloys Compd. 426 (1–2) (2006) 205–212.
[39] F.C. Robles Hernandez, J.H. Sokolowski, Thermal analysis and microscopical characterization of Al-Si hypereutectic alloys, J. Alloys Compd. 419 (1–2) (2006) 180–190.
[40] F.C. Robles Hernandez, J.H. Sokolowski, Effects and on-line prediction of electromagnetic stirring on microstructure refinement of the 319 Al-Si hypoeutectic alloy, J. Alloys Compd. 480 (2) (2009) 416–421.
[41] F.C. Robles Hernández, J.H. Sokolowski, Identification of silicon agglomerates in quenched Al-Si hypereutectic alloys from liquid state, Adv. Eng. Mater. 7 (11) (2005) 1037–1043.
[42] American Railway Engineering and Maintenance-of-Way Association, Manual for Railway Engineering, Mira Digital Pub., St. Louis, MO., 2002 (p. CD-ROMs).
[43] E. Gianotti, Jominy test failures on the steel hardenability evaluation, Metall. Ital. 4 (2008) 43–47.
[44] C.R.N. Nunura, C.A. dos Santos, J.A. Spim, Numerical - experimental correlation of microstructures, cooling rates and mechanical properties of AISI 1045 steel during the jominy end-quench test, Mater. Des. 76 (2015) 230–243.
[45] H. Bhadeshia, R. Honeycombe, Steels: Microstructure and Properties, Elsevier Science, 2011.
[46] G.A. Roberts, R. Kennedy, G. Krauss, Tool Steels, 5th edition ASM International, 1998.
[47] G. Krauss, Steels Processing, Structure, and Performance, ASM International, Materials Park, Ohio, 2015 1 (online resource 704 pages).
[48] 10(2014), A.A, Standard Test Methods for Determining Hardenability of Steel, ASTM International, West Conshohocken, PA, 2014 14.
[49] American Railway Engineering and Maintenance-of-Way Association, Manual for Railway Engineering, Mira Digital Pub., St. Louis, MO., 2002 (p. CD-ROMs).
[50] F. Ziaebrahimi, G. Krauss, Tempered martensite embrittlement in 4130 steel, JOM 33 (9) (1981) A36.
[51] J.P. Materkowski, G. Krauss, Tempered martensite embrittlement in Sae-4340 steel, JOM 31 (12) (1979) 124.